Direct conversion of slow light into a stationary light pulse

Xiao-Jun Zhang,[1,2] Hai-Hua Wang,[1] Cheng-Zhi Liu,[2] Xing-Wei Han,[2] Cun-Bo Fan,[2] Jin-Hui Wu,[1] and Jin-Yue Gao[1,*]

[1]*College of Physics, Jilin University, Changchun 130023, People's Republic of China*

[2]*Changchun Observatory, National Astronomical Observatories, CAS, Changchun 130117, People's Republic of China*

(Received 31 May 2012; published 14 August 2012)

Analysis on direct transforming the slow light into the stationary light pulse (SLP) is presented. Without the process of turning the slow light into the coherence between the lower levels, the generation of SLP is more efficient. The Maxwell-Liouville equations are employed to study the light pulse dynamics in the samples coherently driven by a bichromatic standing wave. The solution indicates that the forward and backward components of the SLP approach to each other exponentially. Such property is described by introducing a quantity called *characteristic length*, which appeared to be the ratio of the optical coherence decay rate and the coefficient of the driving term in Maxwell equation. The necessary length for completing the conversion can be estimated as five times the characteristic length. Several materials are analyzed here, including the ^{87}Rb atoms with different densities, Pr^{3+}-doped yttrium orthosilicate (Pr:YSO), and nitrogen-vacancy color centers in diamond (N-V centers). The values of the characteristic length for the corresponding materials are calculated, as well as the necessary length.

DOI: 10.1103/PhysRevA.86.023821 PACS number(s): 42.50.Gy, 42.70.Qs, 42.50.Hz

I. INTRODUCTION

In the presence of a strong coupling field, an optically dense medium can become transparent and highly dispersive for a weak probe light pulse. Such a phenomenon has been named *electromagnetically induced transparency* (EIT) [1]. The propagation dynamics of probe pulse depends on how the coupling field is arranged. In the case of the constant-amplitude coupling field, the probe pulse which is usually called slow light, travels with a quite low group velocity due to the steep dispersion in the narrow EIT window [2,3]. If the coupling field is adiabatically switching off, the probe pulse can be stored in the medium. During the storage, the electromagnetic component of the pulse completely disappears whereas the quantum state is transformed into the ground-state coherence of the medium. The stored light can be subsequently retrieved by turning the coupling field back on. Such a phenomenon has been explained elegantly using the theory of *dark-state polaritons* [4], and demonstrated in cold sodium cloud [5], vapor of ^{87}Rb atoms [6], and Pr:YSO crystals [7,8].

Instead of the single coupling field, the EIT medium driven by two counterpropagating coupling fields can actually stop the light to create a stationary light pulse (SLP). Unlike the stored light, a SLP is trapped in the medium with the relatively stable electromagnetic components, and can be released by switching one coupling field off. The idea of the SLP is first proposed by André and Lukin [9], and later on the phenomenon was observed in ^{87}Rb vapor maintained at a temperature of 90 °C with the atom number density around 10^{12}–10^{13} cm^{-3}, and the lifetime of SLPs is for about 7 μs [10]. Since the potential application of SLP on nonlinear optics [11–14], Bose-Einstein condensation [15], relativistic effect [16], Tonks-Girardeau gas transition [17], and effective gauge potential [18], SLP has attracted the great attention [19,20]. SLPs can significantly increase the interaction time between the media and the light, therefore, they are very promising for few-photon nonlinear optics [21–24] and quantum information processing [25–27]. The physics underlying of SLP can be understood as the result of balanced multiwave mixing processes [28], $\omega_{p+} - \omega_{c-} + \omega_{c+} \to \omega_{p-}$, and $\omega_{p-} - \omega_{c-} + \omega_{c+} \to \omega_{p+}$. It means that under the effect of forward and backward coupling fields (ω_{c+} and ω_{c-}), SLP can be created as long as the opportunities for the forward and backward photons (ω_{p+} and ω_{p-}) to transform into each other are equal. Such theory has been supported by the experimental observation of the bichromatic SLP in a cloud of cold ^{87}Rb atoms produced by a magneto-optical trap (MOT) [29], and the SLP lasts for about 1.8 μs before converted back into a slow light. The solids such as Pr:YSO and N-V centers are the promising materials for establishing SLPs as well, due to the advantages of the high density of atoms, compactness, absence of atomic diffusion, and simplicity and convenience in preparation and usage. The theoretical prediction of the lifetime of SLP can be 5 μs and 5.7 μs for Pr:YSO and N-V centers, respectively [30]. The formation of SLPs in the medium of nonstationary atoms of low optical depth is also reported [31].

Usually the generation of the SLPs involves the creation of the slow light and the stored light. First, the forward coupling field is on, and the probe pulse travels in the medium as the slow light. Then, the coupling field is switched off and the slow light is converted into the spin coherence of the ground states, which is, as we mentioned before, the stored light. Subsequently, both the forward and backward coupling fields are simultaneously switched on, and the SLP is created. Actually, the creation of the stored light is not necessary for generating the SLP. In other words, the slow light can be converted into SLP directly [32]. To distinguish from the SLP created by building the stored light, we refer to the SLP generated directly from the slow light as *direct stationary light pulse* (DSLP). To our knowledge, there is no particular and detailed investigation that has been done on this phenomenon.

The purpose of the present article is to present a detailed investigation on the creation of DSLP. The general equations for describing the interaction of the laser and the medium are given in Sec. II. Without losing the generality, the bichromatic

[*]jygao@mail.jlu.edu.cn

coupling fields are chosen to interact with the four-level double Λ atomic system of ^{87}Rb. We proceed by giving the numerical and analytic solution of the Maxwell-Liouville equations in Sec. III. The density of the atoms is assumed to be 1.0×10^{10} cm^{-3} which is lower than that in MOT, and the Doppler effect is not considered here. Under several assumptions, the formation process of DSLP is shown as a mathematical expression. The analysis in Sec. III leads to an important property of the medium, namely *characteristic length* for the conversion, which is discussed in Sec. IV. In Sec. V we present our concluding remarks and a brief outlook.

II. THEORETICAL MODE AND BASIC EQUATIONS

We consider an ensemble of double-Λ-type four-level atoms comprising two excited states $|3\rangle$, $|4\rangle$ and two lower states $|1\rangle$ and $|2\rangle$, which represent the hyperfine states $|5P_{3/2}, F' = 1\rangle$, $|5P_{3/2}, F' = 2\rangle$, $|5S_{3/2}, F = 2\rangle$, and $|5S_{3/2}, F = 1\rangle$ of the ^{87}Rb, respectively. As shown in Fig. 1, the coupling field Ω_{c+} (Ω_{c-}) drives the optical transition $|4\rangle \leftrightarrow |2\rangle$ ($|3\rangle \leftrightarrow |2\rangle$), and the probe filed Ω_{p+} (Ω_{p-}) drives the optical transition of $|4\rangle \leftrightarrow |1\rangle$ ($|3\rangle \leftrightarrow |1\rangle$). The symbol $\Omega_{x\pm}(x = c, p)$ defined as $\mu_{ij} E_{x\pm}/2\hbar$ stands for the Rabi frequencies of the corresponding fields. μ_{ij} is the matrix element of the dipole moment between level $|i\rangle$ and $|j\rangle$. $E_{x\pm}$ are the amplitudes of the corresponding fields. We assume that Ω_{c+} and Ω_{c-} are two counterpropagating fields. The probe field Ω_{p+} travels in the same direction as Ω_{c+}. Generally, the traveling direction of Ω_{p-} is determined by the phase matching condition. In our case, it is the same as the direction of Ω_{c-}. The sequences of the coupling fields are shown in Fig. 2. The amplitude of forward coupling field Ω_{c+} maintains constant value, and the backward coupling field Ω_{c-} is switched on at 2 μs. Before switching Ω_{c-} on, the probe pulse Ω_{p+} travels in the sample as a slow light. When Ω_{c-} is turned on, the probe field Ω_{p-} with the opposite wave vector of Ω_{p+} is generated by four-wave mixing, and the DSLP is created.

Before proceeding with our calculations, we would like to present several assumptions to simplify our model: (i) Based on the energy levels shown in Fig. 1, we assume that the wave vectors of the four fields have the same amplitudes. (ii) Most atoms are on the lowest level $|1\rangle$ since the coupling fields are much stronger than the probe pulses. (iii) The coupling field Ω_{c-} is supposed to be temporally modulated smoothly, and the probe field Ω_{p+} has a slowly varying envelope. Under assumptions (i) and (ii), the following equations can be used in the studies of stationary light pulse [30], EIT, as well as slow light and stored light:

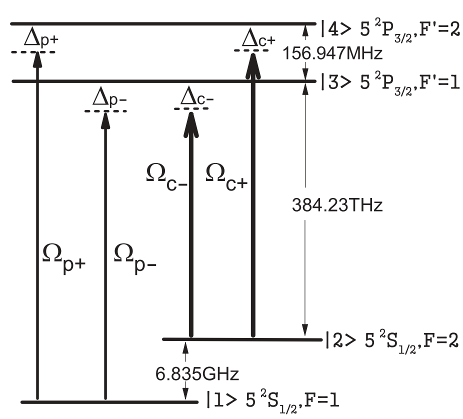

FIG. 1. Schematic level diagram of an ensemble of four-level atoms interacting with two weak probe pulses (Ω_{p+}, Ω_{p-}) and two strong coupling beams (Ω_{c+}, Ω_{c-}).

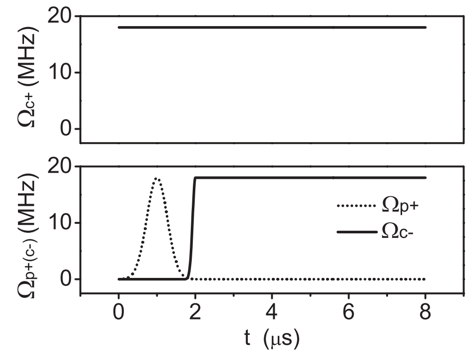

FIG. 2. Sequence of the coupling fields $\Omega_{c\pm}$ and the probe field Ω_{p+}. The forward coupling field Ω_{c+} is always on, and the backward coupling field Ω_{c-} is switched on at 2 μs to form a bichromatic standing wave in the sample.

$$\partial_t \sigma_{41} = i[\sigma_{41}(\Delta_{p+} + i\gamma_{41}) + \sigma_{21}\Omega_{c+} + \Omega_{p+}]; \qquad (1)$$

$$\partial_t \sigma_{31} = i[\sigma_{31}(-\Delta_{c+} + \Delta_{c-} + \Delta_{p+} + i\gamma_{31}) + \sigma_{21}\Omega_{c-} + \Omega_{\text{p-}}]; \qquad (2)$$

$$\partial_t \sigma_{21} = i[\sigma_{21}(-\Delta_{c+} + \Delta_{p+} + i\gamma_{21}) + \sigma_{41}\Omega^*_{c+} + \sigma_{31}\Omega^*_{c-}]; \qquad (3)$$

$$(\partial_t + c\partial_z)\Omega_{p+} = i\, c\gamma_{41}\alpha_+\sigma_{41}/2; \qquad (4)$$

$$(\partial_t - c\partial_z)\Omega_{p-} = i\, c\gamma_{31}\alpha_-\sigma_{31}/2, \qquad (5)$$

where $\alpha_+ = \ell\mu^2_{41}k_{p+}/\gamma_{41}$, $\alpha_- = \ell\mu^2_{31}k_{p-}/\gamma_{31}$, and $\ell = N_0/\varepsilon_0$. The parameter γ_{ij} denotes the coherence decay rate of the transition $|i\rangle \leftrightarrow |j\rangle$, and $\Delta_{x\pm}(x = c, p)$ denote the detunings of the corresponding fields as shown in Fig. 1. In addition, we have adopted the phase matching condition $\Delta_{p-} = -\Delta_{c+} + \Delta_{c-} + \Delta_{p+}$ in Eqs. (1)–(3). Notice that Eqs. (1)–(3) are not all of the density element equations. This is because the off-diagonal density elements σ_{43}, σ_{32}, and σ_{42} are neglectable according to assumption (ii).

III. THE GENERATION OF DIRECT STATIONARY LIGHT PULSE

In this section, we use the theoretical approach developed in the previous section to investigate the DSLP generation in the cold thermal ^{87}Rb sample where the residual Doppler broadening is negligible. The atomic polarizations can be written as $\sigma^{(1)}_{41} = i\,(A_1\Omega_{p+} + A_2\Omega_{p-} + A_3\dot{\Omega}_{p+} + A_4\dot{\Omega}_{p-})$ and $\sigma^{(1)}_{31} = i\,(B_1\Omega_{p+} + B_2\Omega_{p-} + B_3\dot{\Omega}_{p+} + B_4\dot{\Omega}_{p-})$, calculated in the appendix. The superscripts $^{(1)}$ stand for the *first order solutions* of the off-diagonal density elements which are good enough for describing the polarization of the atoms [4]. Then the wave

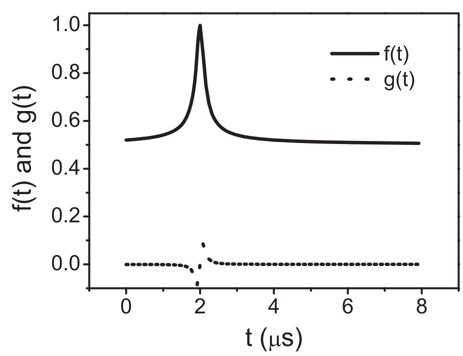

FIG. 3. Numerical calculation of the time-varying components of the parameter A_1: $f(t)$ and $g(t)$. All of the detunings are set as zeros, and the other parameters are $\gamma = 2\pi \times 6$ MHz and $\gamma_0 = 2\pi \times 1$ kHz. The forward coupling Rabi frequency is set as $\Omega_{c+} = 20$ MHz, and backward coupling Rabi frequency is chosen to be $\Omega_{c-}(t) = 20/\pi \arctan[8 \times 10^6(t - 2 \times 10^{-6})]$ MHz.

equations can be written as

$$(1 + c\beta A_3)\,\partial_t\Omega_{p+} + c\partial_z\Omega_{p+} = -c\beta(A_1\Omega_{p+} + A_2\Omega_{p-} + A_4\partial_t\Omega_{p-}), \tag{6}$$

$$(1 + c\beta B_4)\,\partial_t\Omega_{p-} - c\partial_z\Omega_{p-} = -c\beta(B_1\Omega_{p+} + B_2\Omega_{p-} + B_3\partial_t\Omega_{p+}). \tag{7}$$

The parameter β is given by the expression,

$$\beta = \ell\mu^2 k/(2\hbar). \tag{8}$$

Note that the β we introduced here is related to the assumption: $k_{p+} \simeq k_{p-} = k$ and $\mu_{41} \simeq \mu_{31} = \mu$. In our case $\beta = 9.27 \times 10^9\ \mathrm{m^{-1}\,s^{-1}}$. For the ^{87}Rb atoms, the coherence decay rates of the optical transitions are of the same order of magnitude ($2\pi \times 6$ MHz); so are the coherence decay rates of the spin transitions ($2\pi \times 1$ kHz). Regarding the above characteristic of the system, we introduce two parameters γ and γ_0 for simplification:

$$\gamma = \gamma_{41} = \gamma_{31} = \gamma_{42} = \gamma_{32}, \tag{9}$$

$$\gamma_0 = \gamma_{43} = \gamma_{21}. \tag{10}$$

However, the coefficients $A_i, B_i (i = 1,2,3,4)$ are still quite complex. Considering that $\Omega_{c\pm} \gg \Omega_{p\pm}, \gamma \gg \gamma_0$, the terms of A_i, B_i which are proportional to $\partial_t\Omega_{c-}(t)$ can be neglected. For example, after treating all the detunings as zero, and all Rabi frequencies real numbers, the expression of A_1 can be written as

$$A_1 = \gamma^{-1}\left[1 - f(t) + g(t)\right], \tag{11}$$

where

$$f(t) = \frac{\Omega_{c+}^2}{\gamma\gamma_0 + \Omega_{c+}^2 + \Omega_{c-}^2(t)}, \tag{12}$$

$$g(t) = \frac{\gamma\Omega_{c+}^2\Omega_{c-}(t)\cdot\partial_t\Omega_{c-}(t)}{\left[\gamma\gamma_0 + \Omega_{c+}^2 + \Omega_{c-}^2(t)\right]^3}. \tag{13}$$

As shown in Fig. 3, $g(t)$ is much smaller than $f(t)$ for all the values of t, so it is neglectable. Based on our calculation, such an operation can be applied to the other coefficients $A_i, B_i (i = 2,3,4)$ as well. The physical reason of $g(t) \ll f(t)$ is that $\Omega_{c-}(t)$ varies slow and smooth enough to avoid the nonadiabatic coupling of the "dark" and "bright" states [33]. Actually, this condition is quite weak: As we can see from Eq. (13) $g(t) \sim \partial_t\Omega_{c-}/8\Omega_{c+}^2$. This means that the backward coupling field can jump up from zero to 20 MHz in 0.05 μs without violating the condition. Therefore, $A_i, B_i (i = 1,2,3,4)$ can be rewritten as

$$\begin{aligned}
A_1 &= i\gamma^{-1} - i\Omega_{c+}^2\gamma^{-2}\xi^{-1};\\
A_2 &= -i\Omega_{c+}\Omega_{c-}\gamma^{-2}\xi^{-1};\\
A_3 &= i\Omega_{c+}^2\gamma^{-2}\xi^{-2};\\
A_4 &= i\Omega_{c+}\Omega_{c-}\gamma^{-2}\xi^{-2};\\
B_1 &= -i\Omega_{c+}\Omega_{c-}\gamma^{-2}\xi^{-2};\\
B_2 &= i\gamma^{-1} - i\Omega_{c-}^2\gamma^{-2}\xi^{-1};\\
B_3 &= i\Omega_{c+}\Omega_{c-}\gamma^{-2}\xi^{-2};\\
B_4 &= i\Omega_{c-}^2\gamma^{-2}\xi^{-2}.
\end{aligned}$$

Here we introduce a parameter $\xi = \gamma_0 + \Omega_{c+}\gamma^{-1} + \Omega_{c-}\gamma^{-1}$ to simplify the above expressions. To solve partial differential Eqs. (6) and (7), we assume that the forward and backward pulses can be written as $\Omega_{p+} = T(t)f_+(z)$, and $\Omega_{p-} = T(t)f_-(z)$. The solution will strongly depend on the initial and the boundary condition. However, we set the time derivative of $T(t)$ to be zero which means that the pulses are treated as the plane wave. In other words, we assume that the bandwidth of the pulse is very narrow. The consequence of this assumption is that the model does not include the decay and the diffusion process any more. Then the wave equations can be easily obtained:

$$\frac{a_+a_-\beta\gamma f_- - \beta(\gamma_0 + a_-^2\gamma)f_+}{\gamma(\gamma_0 + (a_+^2 + a_-^2)\gamma)} = \frac{\partial f_+}{\partial z}, \tag{14}$$

$$\frac{a_+a_-\beta\gamma f_+ - \beta(\gamma_0 + a_+^2\gamma)f_-}{\gamma(\gamma_0 + (a_+^2 + a_-^2)\gamma)} = \frac{\partial f_-}{\partial z}. \tag{15}$$

Here $a_+ = f_+/\gamma, a_- = f_-/\gamma$. By introducing two parameters $M = a_+a_-$ and $R = a_-/a_+$, the above equations can be changed into the form,

$$\frac{\beta}{\gamma} \times \frac{\gamma f_- - \left(\frac{\gamma_0}{M} + \gamma R\right)f_+}{\frac{\gamma_0}{M} + (R + R^{-1})\gamma} = \frac{\partial f_+}{\partial z}, \tag{16}$$

$$\frac{\beta}{\gamma} \times \frac{\gamma f_+ - \left(\frac{\gamma_0}{M} + \gamma R^{-1}\right)f_-}{\frac{\gamma_0}{M} + (R + R^{-1})\gamma} = \frac{\partial f_-}{\partial z}. \tag{17}$$

Equations (16) and (17) are our main result and can be used to analyze the DSLP. Here we would like to give a careful discussion on these two equations. First, the equations can only describe the situation when the backward coupling field is switched at 2 μs shown in Fig. 2. Otherwise, $R^{-1} \to \infty$ and the equations become unreasonable. Second, when the amplitudes of the two coupling fields are identical ($R = 1$), f_+ and f_- can become stable with respect to z if the following algebraic equations are satisfied.

$$\begin{cases} \gamma f_- - \left(\frac{\gamma_0}{M} + \gamma\right)f_+ = 0,\\ \gamma f_+ - \left(\frac{\gamma_0}{M} + \gamma\right)f_- = 0. \end{cases} \tag{18}$$

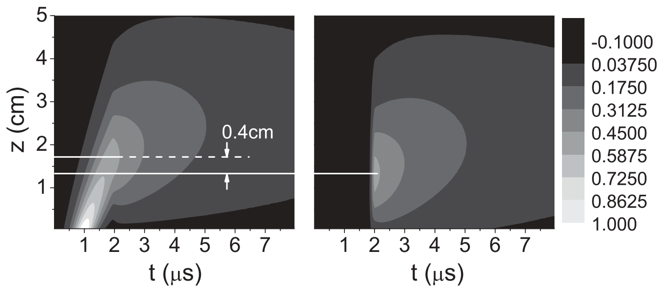

FIG. 4. Numerical simulation of the DSLP in ^{87}Rb. The coupling fields sequences are shown in Fig. 2. The incident probe pulse is assumed to have a Gaussian profile $I_p = I_{p0}\exp[-(t-t_0)^2/\tau^2]$ with $t_0 = 1\ \mu$s and duration $\tau = 0.375\ \mu$s. The probe and coupling detunings are set as $\Delta_{p\pm} = \Delta_{c\pm} = 0$. The other common parameters are $\gamma_{41} = \gamma_{31} = 2\pi \times 6$ MHz, $\gamma_{21} = 2\pi \times 1$ kHz, $d_{31} = 1.465 \times 10^{-29}$ C m, $N_0 = 1.0 \times 10^{10}$ cm^{-3}, $k_p = 2\pi/(780$ nm).

If the DSLP is created, f_+ and f_- should be equal for all values of z, so it must be true that $\gamma_0/M \ll \gamma$. This is just another way to write the condition of $\Omega_\pm \gg \sqrt{\gamma\gamma_0}$ which is required in the EIT demonstration, creation of the slow light, and stored light. When the term of γ_0/M is neglected in Eqs. (16) and (17), it is clear that the ratio of the coupling field amplitudes plays an important role in the propagation dynamics of the pulse. Such a characteristic is quite similar with the dark-state polaritons [4] and the pulse matching phenomenon [38].

Before proceeding to the next section, we would like to present the numerical solution of the DSLP by solving Eqs. (1)–(5); the results of Ω_{p+} and Ω_{p-} are given in Fig. 4. As we can see that the pulses stop in the medium when the backward coupling is turned on at 2 μs. One special characteristic is that the stationary light pulse is not formed immediately when the backward coupling field Ω_{c-} is turned on. As we can see the Ω_{p+} and Ω_{p-} are not exactly the same after 2 μs. The two components deviate from each other at about 0.4 cm in the medium. This is because when the Ω_{c-} is just switched on, the number of forward photons is larger than that of the backward ones, therefore Ω_{p+} is still moving forward until the numbers of the forward and backward photons are equal.

IV. CHARACTERISTIC LENGTH OF MEDIUM

As we mentioned before, during the formation process of the DSLP, the two components deviate from each other for a small distance, which is called the *characteristic length* of the medium in the following discussion. The analytic solutions of the ordinary differential Eqs. (16) and (17) can be used to reveal such a property of the medium. And they can be easily obtained:

$$f_+(z) = \frac{1}{R+R^{-1}} e^{-\frac{t^2}{\tau^2}-\frac{z\beta}{\gamma}} [R^{-1}\mathcal{E}(R,M) + R], \tag{19}$$

$$f_-(z) = \frac{1}{R+R^{-1}} e^{-\frac{t^2}{\tau^2}-\frac{z\beta}{\gamma}} [\mathcal{E}(R,M) - 1]M, \tag{20}$$

where

$$\mathcal{E}(R,M) = \exp\left[\frac{(R+R^{-1})\beta z}{\frac{\gamma_0}{M} + (R+R^{-1})\gamma}\right]. \tag{21}$$

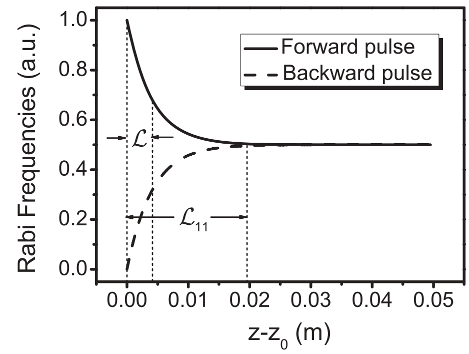

FIG. 5. The amplitude peaks of the two components ($\Omega_{p\pm}$) as the function of z. $z_0 = 1.5$ cm is the position of the forward pulse peak when the backward coupling field is switched on. $\mathcal{L}$ is the characteristic length of the medium, which equals 4.07 mm. $\mathcal{L}_{11}$ can be considered the distance that the two components must travel to become equal to each other. The parameters used here are identical with those in Fig. 4.

The terme^{-t^2/τ^2} is brought in as the constant respecting to z by solving the differential Eqs. (16) and (17). Here, τ can be regarded as the pulse width of slow light when the backward coupling field is switched on. We would like to discuss a typical situation here: Without violating the condition of $g(t) \ll f(t)$, the backward coupling field is quickly turned on, and it "covers" the medium immediately because the coupling field travels much faster than the slow light pulse. Anyway, the above discussion leads to $R = 1$ for $t > 2\ \mu$s. We further change M into M_ϵ to represent the production of the two equal coupling field amplitudes. Then, the expressions for the two components become

$$f_+(z) = \tfrac{1}{2} e^{-\frac{t^2}{\tau^2}-\frac{\beta z}{\gamma}} \left\{1 + \exp\left[\frac{\beta z}{(\gamma_0/2M_\epsilon)+\gamma}\right]\right\}, \tag{22}$$

$$f_-(z) = \tfrac{1}{2} e^{-\frac{t^2}{\tau^2}-\frac{\beta z}{\gamma}} \left\{\exp\left[\frac{\beta z}{(\gamma_0/2M_\epsilon)+\gamma}\right] - 1\right\}. \tag{23}$$

Figure 5 shows the peaks of pulse amplitudes as a function of z. The data are obtained from Eqs. (22) and (23). The parameter z_0 (shown in Fig. 5) stands for the position of the forward pulse's peak when the backward coupling fields are just switched on, in our case, $z_0 = 1.5$ cm. The time dependence of the pulses is hid to emphasize the relation between the peaks of the pulses and z. As we can see the two components travel about 2 cm through the medium and become equal to each other. To describe such behavior, we try to solve the equation $f_+(z) = f_-(z)$. Based on our calculation, the above equations can be reduced to $\exp(-\beta z/\gamma) = 0$, which indicates that the characteristic length of the medium is

$$\mathcal{L} = \frac{\gamma}{\beta}. \tag{24}$$

Using the parameters listed in Fig. 4, we estimate that the characteristic length of ^{87}Rb vapor is about 4.07 mm which is consistent with the numerical simulation. It is necessary to emphasize that such a result highly depends on the density of the atoms which is 1.0×10^{10} cm^{-3} here.

As we can see the characteristic length of the medium depends on the coherence decay rate of the optical transition and the coefficient of the driving term in the Maxwell equation. To our knowledge, the experimentally supported [29] model where SLPs can be understood is the multiwave mixing process [12,28]. Establishing SLPs is actually the process of forcing the forward and backward photons to transform into each other, for example, in our case, the photons of Ω_{p+} can take the path of $|1\rangle \to |4\rangle \to |2\rangle \to |3\rangle \to |1\rangle$ to become the photons of Ω_{p-}, and the backward photons can take the reverse way to transform into the forward ones. Apparently, the coherence decay rate γ plays an important role in such a process. The large γ will cause the longer characteristic length of the medium.

The parameter β is the coefficient of the polarization in the Maxwell equations [see Eqs. (6)–(8)]. The larger β indicates that the interaction between the laser and atoms is stronger and the laser fields seem more animated to interact with the atoms. This also means that the transformation of the forward and backward photons proceed more quickly which leads to the smaller characteristic length.

Note that the characteristic length is quite similar to the optical depth $\tau_{\rm od}$, quantitatively, $\mathcal{L} = \tau_{\rm od}^{-1} V/A$. Where V denotes the volume that the laser beam occupies in the sample, and A is the cross section of the beam. As a measure of transparency, optical depth is defined by the negative natural logarithm of the fraction of radiation that is not scattered or absorbed on a path. In other words, optical depth describes how strong the atoms can absorb or interact with the light. Clearly, the larger optical depth will lead to the smaller characteristic length when the medium is not absorbing the light but only changing the direction of the light propagation. Although the pulses are treated as the electromagnetic wave here, the characteristic length can still be interpreted from the quantum view: If the initial number of the forward photons is n, then only ne^{-1} photons are *not* converted into the backward ones after traveling the distance $\mathcal{L}$. So $\mathcal{L}$ can be regarded as a measure of such conversion.

The characteristic length cannot be taken as the necessary length that the two components have to travel before they equal each other. Based on our calculation, the necessary distance can be obtained by solving the following equation:

$$\sum_{n=1}^{11} \frac{\left[\partial_\xi^{n-1} e^{-\xi/\mathcal{L}}\right]_{\xi=\mathcal{L}} (x-\mathcal{L})^{n-1}}{(n-1)!} = 0. \tag{25}$$

For the parameters listed in Fig. 4, the above equation leads to $z = \mathcal{L}_{11} = 0.0199$ m for ^{87}Rb with density of 1.0×10^{10} cm^{-3}, which is nearly five times of the characteristic length.

Normally, when the phenomena based on EIT, including SLP, are investigated, the probe and coupling beams intersect at the small crossing angle, for example, 0.3° in Ref. [29], about 30 mrad in Ref. [36]. Clearly, only the laser overlapping part of the medium contributes to the interaction. The characteristic length gives us a standard of how the crossing angle can be arranged. For example, for the ^{87}Rb vapor with the density of 1.0×10^{10} cm^{-3}, the coupling beam focused to a e^{-2} full width D_0 of 100 μm, the crossing angle of the coupling fields and the probe pulse should not be larger than $\arcsin(D_0/\mathcal{L})$, which is about 5 mrad.

TABLE I. Parameters for the characteristic length of Pr:YSO, N-V center crystals, and ^{87}Rb in MOT. The data of ^{87}Rb in MOT are from Ref. [32] and the data of Pr:YSO and N-V center crystals can be found in Ref. [35]. The dagger (†) marked values are actually not calculated directly from the given value of γ and β. For such solid materials, the inhomogeneous broadening must be taken into account. If the lineshape of the distribution of the ions is modeled as the Lorentzian function, the total decoherent rate can be written as the sum of the broadening width and γ [30]. Considering the optical repump scheme is used in the experimental demonstration, the broadening width should be replaced by the laser linewith, which is chosen as 1 MHz here. The ion density is also affected. The details can be found in Ref. [35].

	$\gamma/2\pi$ (Hz)	β (m^{-1}s^{-1})	$\mathcal{L}$ (mm)
^{87}Rb	3.0×10^6	7.27×10^9	2.5
Pr:YSO	9.0×10^3	1.35×10^9	0.75†
N-V centers	3.0×10^8	1.05×10^{12}	0.29†

If the wave vectors of all the fields are parallel, the length of the medium should be considered carefully, because the spatial pulse length of the slow light should be smaller than the length of the medium. Assuming that the light pulse with the width τ_t can be delayed for δ_d in the sample of which the length is l, in order to generate the DSLP, the sample should have the length larger than

$$L = \frac{cl}{l + c\delta_d}\tau_t + \mathcal{L}_{11}. \tag{26}$$

Next, we would like to extend our calculation into some other materials, such as ^{87}Rb in MOT, Pr:YSO, and N-V center crystals. Table I shows the characteristic lengths of those mediums for establishing SLPs. For the ^{87}Rb in MOT, the atomic density, normally 1.3×10^{11} cm^{-3} [29,34], is much larger than the atomic vapor that we focus on before; therefore, the characteristic length is shorter than the atomic vapor.

For the solid materials, the inhomogeneous broadenings should be take into account and lead to a large coherence decay rate [30]. In addition, the density of the ions depends on the laser linewidth [35] which is assumed to be 1 MHz in the calculation for both Pr:YSO and N-V centers. In Pr:YSO, the value of $\mathcal{L}_{11}$ is about 3.68 mm, and D_0 is normally 100 μm; the crossing angle of the coupling and probe beams should not be larger than 27 mrad. If the parallel traveling fields are used, the sample length should not be less than 6.9 mm.[1] For N-V centers, with the same D_0, the maximal cross angle of the fields is 75 mrad. Because of the lack of experimental data on the group velocity, the minimal length of the crystal is not calculated. However, based on the work of Scully and coworkers [35], the group velocity in N-V center crystals should be less than that in Pr:YSO. Such a result indicates that the sample length of N-V center crystals can be smaller as compared with that in Pr:YSO.

[1]The group velocity depends on the laser power of the coupling field which is about 3 mW here [37].

V. CONCLUSIONS

In summary, we have presented a detailed study on the direct transformation of slow light into the stationary light pulse in a four-level atomic system driven by the bichromatic standing wave coupling field. By switching on the backward coupling field, the slow light pulse will interact with the "dressed" atoms to became the stationary light pulse. Using the parameters of ^{87}Rb, the numerical simulation is presented and shows that the stationary light pulse is not established immediately after the backward coupling field is turned on. Such a phenomenon is quite understandable using the multiwave mixing process. By solving the Maxwell-Liouville equation analytically, the characteristic length of the medium is introduced to describe such spatial delay. As we can see from Eq. (24), the characteristic length takes a quit simple form and only relates to two parameters β and γ. Since the β is determined by the density of the atoms, the characteristic length is quite sensitive to the density as well. Four kinds of medium are studied here, such as cold ^{87}Rb with lower density, ^{87}Rb in MOT, Pr:YSO, and N-V center crystals, the corresponding values of the characteristic length are 4.07, 2.5, 0.75, and 0.29 mm, respectively.

The characteristic length has two important implications: First, the crossing angle of the coupling field and probe pulses has a limit. Second, the characteristic length can give us a standard for the medium length to complete the direct conversion from the slow light into the stationary light pulse. Based on our analysis, the necessary length ($\mathcal{L}_{11}$) of the medium can be calculated from Eq. (25). For all the medium we studied, the value of the $\mathcal{L}_{11}$ is roughly five times the characteristic length.

ACKNOWLEDGMENTS

The authors would light to acknowledge financial support from the National Basic Research Program of the People's Republic of China (Grant No. 2011CB921603) and the National Natural Science Foundation of China (Grants No. 11074097, No. 10904048, No. 11073033, and No. 11103047).

APPENDIX

The numerical solution of the essential density Eqs. (1)–(3) is presented here. First of all, we treat the $\partial_t \rho_{i1} = 0, (i = 2,3,4)$ to get the zero order solutions, which are

$$\sigma_{41}^{(0)} = i\kappa_{41}(\sigma_{21}\Omega_{c+} + \Omega_{p+}), \tag{A1}$$

$$\sigma_{31}^{(0)} = i\kappa_{31}(\sigma_{21}\Omega_{c-} + \Omega_{p-}), \tag{A2}$$

$$\sigma_{21}^{(0)} = \frac{\kappa_{41}^{-1}\Omega_{c+}\Omega_{p+} + \kappa_{31}^{-1}\Omega_{c-}\Omega_{p-}}{-\kappa_{21} - \kappa_{41}^{-1}\Omega_{c+}^2 - \kappa_{31}^{-1}\Omega_{c-}^2}. \tag{A3}$$

To simplify the expressions, the space and time dependence of the Rabi frequencies is not indicated. Three complex parameters are defined here as $\kappa_{41} = \gamma_{41} - i\Delta_{p+}, \kappa_{31} = \gamma_{31} + i(\Delta_{c+} - \Delta_{c-} - \Delta_{p+}), \kappa_{21} = \gamma_{21} + i(\Delta_{c+} - \Delta_{p+})$.

The first order solution of σ_{21} can be obtained by substituting Eq. (A3) into the left-hand side of Eq. (3), which is

$$\begin{aligned}\sigma_{21}^{(1)} = -\left(\kappa_{21} + \frac{\Omega_{c+}^2}{\kappa_{41}} + \frac{\Omega_{c-}^2}{\kappa_{31}}\right)^{-1} &\times \big\{\Omega_{c+}\Omega_{p+}\kappa_{41}^{-1} + \Omega_{c-}\Omega_{p-}\kappa_{31}^{-1} \\ &+ \big\{2\kappa_{41}\Omega_{c-}(\kappa_{31}\Omega_{c+}\Omega_{p+} + \kappa_{41}\Omega_{c-}\Omega_{p-})\dot{\Omega}_{c-} \\ &- \big[\kappa_{31}(\kappa_{21}\kappa_{41} + \Omega_{c+}^2) + \kappa_{41}\Omega_{c-}^2\big] \\ &\times [\kappa_{31}\Omega_{c+}\dot{\Omega}_{p+} + \kappa_{41}(\Omega_{p-}\dot{\Omega}_{c-} + \Omega_{c-}\dot{\Omega}_{p-})]\big\} \\ &\times \big[\kappa_{31}(\kappa_{21}\kappa_{41} + \Omega_{c+}^2) + \kappa_{41}\Omega_{c-}^2\big]^2\big\}.\end{aligned} \tag{A4}$$

Here $\dot{\Omega}$ denotes the time derivative of Ω. Notice that $\dot{\Omega}_{c+} = 0$ as shown in Fig. 2. Then the first-order solution of σ_{41} and σ_{31} can be obtained by substituting Eq. (A4) into Eqs. (A1) and (A2), which can be written as $\sigma_{41}^{(1)} = A_1\Omega_{p+} + A_2\Omega_{p-} + A_3\dot{\Omega}_{p+} + A_4\dot{\Omega}_{p-}$ and $\sigma_{31}^{(1)} = B_1\Omega_{p+} + B_2\Omega_{p-} + B_3\dot{\Omega}_{p+} + B_4\dot{\Omega}_{p-}$, where

$$A_1 = \frac{i\left(\beta_-\phi^2 - 2\kappa_{31}^2\kappa_{41}\Omega_{c+}^2\Omega_{c-}\dot{\Omega}_{c-}\right)}{\phi^3}; \tag{A5}$$

$$A_2 = \frac{-i\Omega_{c+}\left(\Omega_{c-}\phi^2 - \kappa_{31}\kappa_{41}\varphi\dot{\Omega}_{c-}\right)}{\phi^3}; \tag{A6}$$

$$B_1 = \frac{-i\Omega_{c+}\Omega_{c-}\left(\phi^2 + 2\kappa_{31}\kappa_{41}^2\Omega_{c-}\dot{\Omega}_{c-}\right)}{\phi^3}; \tag{A7}$$

$$B_2 = \frac{i\left(\beta_+\phi^2 + \kappa_{41}^2\Omega_{c-}\varphi\dot{\Omega}_{c-}\right)}{\phi^3}; \tag{A8}$$

$$A_3 = \frac{i\kappa_{31}^2\Omega_{c+}^2}{\phi^2}; \tag{A9}$$

$$A_4 = \frac{i\kappa_{31}\kappa_{41}\Omega_{c+}\Omega_{c-}}{\phi^2}; \tag{A10}$$

$$B_3 = \frac{i\kappa_{31}\kappa_{41}\Omega_{c+}\Omega_{c-}}{\phi^2}; \tag{A11}$$

$$B_4 = \frac{i\kappa_{41}^2\Omega_{c-}^2}{\phi^2}. \tag{A12}$$

Four parameters are introduced here to simplify the above expressions, which are

$$\phi = \kappa_{31}\left(\kappa_{21}\kappa_{41} + \Omega_{c+}^2\right) + \kappa_{41}\Omega_{c-}^2;$$

$$\varphi = \kappa_{31}\left(\kappa_{21}\kappa_{41} + \Omega_{c+}^2\right) - \kappa_{41}\Omega_{c-}^2;$$

$$\beta_+ = \kappa_{21}\kappa_{41} + \Omega_{c+}^2;$$

$$\beta_- = \kappa_{21}\kappa_{31} + \Omega_{c-}^2.$$

[1] S. E. Harris, Phys. Today **50**, 36 (1997).
[2] L. V. Hau, S. E. Harris, Z. Dutton, and C. H. Behroozi, Nature (London) **397**, 594 (1999).
[3] M. M. Kash, V. A. Sautenkov, A. S. Zibrov, L. Hollberg, G. R. Welch, M. D. Lukin, Y. Rostovtsev, E. S. Fry, and M. O. Scully, Phys. Rev. Lett. **82**, 5229 (1999).

[4] M. Fleischhauer and M. D. Lukin, Phys. Rev. Lett. **84**, 5094 (2000).
[5] C. Liu, Z. Dutton, C. H. Behroozi, and L. V. Hau, Nature (London) **409**, 490 (2001).
[6] D. F. Phillips, A. Fleischhauer, A. Mair, R. L. Walsworth, and M. D. Lukin, Phys. Rev. Lett. **86**, 783 (2001).
[7] A. V. Turukhin, V. S. Sudarshanam, M. S. Shahriar, J. A. Musser, B. S. Ham, and P. R. Hemmer, Phys. Rev. Lett. **88**, 023602 (2001).
[8] J. J. Longdell, E. Fraval, M. J. Sellars, and N. B. Manson, Phys. Rev. Lett. **95**, 063601 (2005).
[9] A. André and M. D. Lukin, Phys. Rev. Lett. **89**, 143602 (2002).
[10] M. Bajcsy, A. S. Zibrov, and M. D. Lukin, Nature (London) **426**, 638 (2003).
[11] A. André, M. Bajcsy, A. S. Zibrov, and M. D. Lukin, Phys. Rev. Lett. **94**, 063902 (2005).
[12] S. A. Moiseev and B. S. Ham, Phys. Rev. A **73**, 033812 (2006).
[13] S. A. Moiseev, Y. Chen, and B. S. Ham, J. Korean Phys. Soc. **49**, 2293 (2006).
[14] X. J. Liu, X. Liu, Z. X. Liu, L. C. Kwek, and C. H. Oh, Phys. Rev. A **75**, 023809 (2007).
[15] M. Fleischhauer, J. Otterbach, and R. G. Unanyan, Phys. Rev. Lett. **101**, 163601 (2008).
[16] J. Otterbach, R. G. Unanyan, and M. Fleischhauer, Phys. Rev. Lett. **102**, 063602 (2009).
[17] D. E. Chang, V. Gritsev, G. Morigi, V. Vuletić, M. D. Lukin, and E. A. Demler, Nat. Phys. **4**, 884 (2008).
[18] J. Otterbach, J. Ruseckas, R. G. Unanyan, G. Juzeliūnas, and M. Fleischhauer, Phys. Rev. Lett. **104**, 033903 (2010).
[19] Jin-Hui Wu, M. Artoni, and G. C. La Rocca, Phys. Rev. A **81**, 033822 (2010).
[20] Jin-Hui Wu, M. Artoni, and G. C. La Rocca, Phys. Rev. A **82**, 013807 (2010).
[21] S. E. Harris and Y. Yamamoto, Phys. Rev. Lett. **81**, 3611 (1998); S. E. Harris and L. V. Hau, *ibid.* **82**, 4611 (1999).
[22] H. Schmidt and A. Imamolu, Opt. Lett. **21**, 1936 (1996).
[23] M. D. Lukin and A. Imamoğlu, Phys. Rev. Lett. **84**, 1419 (2000).
[24] A. S. Zibrov, M. D. Lukin, and M. O. Scully, Phys. Rev. Lett. **83**, 4049 (1999).
[25] M. Fleischhauer, S. F. Yelin, and M. D. Lukin, Opt. Commun. **179**, 395 (2000).
[26] M. D. Lukin, S. F. Yelin, and M. Fleischhauer, Phys. Rev. Lett. **84**, 4232 (2000).
[27] A. E. Kozhekin, K. Mølmer, and E. Polzik, arXiv:cond-mat/9912014.
[28] S. A. Moiseev and B. S. Ham, Opt. Spectrosc. **103**, 210 (2007).
[29] Yen-Wei Lin, Wen-Te Liao, Thorsten Peters, Huang-Chih Chou, Jian-Siung Wang, Hung-Wen Cho, Pei-Chen Kuan, and Ite A. Yu, Phys. Rev. Lett. **102**, 213601 (2009).
[30] Xiao-Jun Zhang, Hai-Hua Wang, Lei Wang, Ren-Gang Wan, Jun Kou, Yun-Fei Fan, Bing Zhang, and Jin-Yue Gao, Phys. Rev. A **83**, 063804 (2011).
[31] Thorsten Peters, Shih-Wei Su, Yi-Hsin Chen, Jian-Siung Wang, Shih-Chuan Gou, and Ite A. Yu, Phys. Rev. A **85**, 023838 (2012).
[32] Yen-Wei Lin, Hung-Chih Chou, Thorsten Peters, Wen-Te Liao, Hung-Wen Cho, Pei-Chen Guan, and Ite A. Yu, arXiv:0810.0903v1.
[33] M. Fleischhauer and A. S. Manka, Phys. Rev. A **54**, 794 (1996).
[34] Yen-Wei Lin, Hung-Chih Chou, Prashant P. Dwivedi, Ying-Cheng Chen, and Ite A. Yu, Opt. Express **16**, 3753 (2008).
[35] Elena Kuznetsova, Olga Kocharovskaya, Philip Hemmer, and Marlan O. Scully, Phys. Rev. A **66**, 063802 (2002).
[36] Byoung S. Ham and Joonsung Hahn, Opt. Express **34**, 776 (2009).
[37] Hai-Hua Wang, Ai-Jun Li, Dun-Mao Du, Yun-Fei Fan, Lei Wang, Zhi-Hui Kang, Yun Jiang, Jin-Hui Wu, and Jin-Yue Gao, Appl. Phys. Lett. **93**, 221112 (2008).
[38] S. E. Harris, Phys. Rev. Lett. **70**, 552 (1993).